THE JOURNAL OF PHYSICAL CHEMISTRY LETTERS
A JOURNAL OF THE AMERICAN CHEMICAL SOCIETY

pubs.acs.org/JPCL
Letter

A First Proposal on the Nitrobenzene Photorelease Mechanism of NO_2 and Its Relation to NO Formation through a Roaming Mechanism

Angelo Giussani* and Graham A. Worth

Cite This: J. Phys. Chem. Lett. 2024, 15, 2216−2221

ABSTRACT: Despite the fact that NO_2 is considered to be the main photoproduct of nitrobenzene photochemistry, no mechanism has ever been proposed to rationalize its formation. NO photorelease is instead a more studied process, probably due to its application in the drug delivery sector and the study of roaming mechanisms. In this contribution, a photoinduced mechanism accounting for the formation of NO_2 in nitrobenzene is theorized based on CASPT2, CASSCF, and DFT electronic structure calculations and CASSCF classical dynamics. A triplet $n\pi^*$ state is shown to evolve toward C−NO_2 dissociation, being, in fact, the only low-lying excited state favoring such a deformation. Along the triplet dissociation path, the possibility to decay to the singlet ground state results in the frustration of the dissociation and in the recombination of the fragments, either back to the nitro or the nitrite isomer. The thermal decomposition of the latter to NO constitutes globally a roaming mechanism of NO formation.

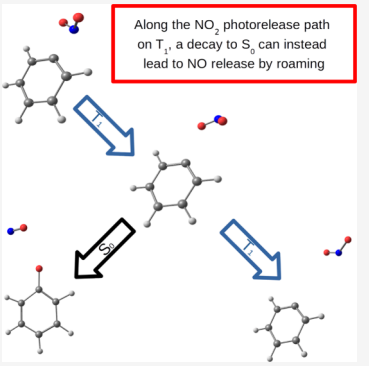

Nitrobenzene has recently attracted a lot of attention in the photophysical and photochemical community.[1−7] This is easily understandable due, from one side, to its representative role in the nitroaromatic family and, from the other side, to its peculiar photoinduced dynamics. The nitrobenzene photoresponse is in fact intrinsically key for basis science, displaying an unusual, for pure organic systems, ultrafast decay into the triplet manifold and a wide variety of photoinduced reactions. Moreover, its photochemistry has important applications in the energetic materials sector, in the study of urban atmospheric contaminants, and in the drug delivery sector.[8−10]

Nitrobenzene can photorelease NO_2, NO, and O.[11] The efficiency of these photoreactions is low, and no values for the quantum yields have been reported, as far as we know. It is generally considered that the formation of O is the least relevant path, while two experimental studies from Galloway et al. and Lee, Ni, and co-workers performing vacuum-ultraviolet photoionization mass spectrometry and multimass ion imaging techniques, respectively, have reported that NO_2 is always produced in higher quantities than NO and that the formation of NO_2 is even more favored at higher excitation energies.[11,12] Such a vision has, however, been challenged by ultrafast electron diffraction measurements by Zewail and co-workers, who concluded that NO is instead the main result of nitrobenzene photochemistry.[13] Despite its importance, the mechanism of NO_2 photorelease has received very little attention, and there is no generally accepted mechanism.

The photoformation of NO has been instead the subject of various experimental and theoretical works.[12−16] One of the most intriguing results was the determination of a bimodal distribution of the translational energy of the photoreleased NO molecules. This was first characterized by Lee, Ni, and co-workers[12] and later reconfirmed by Suits and co-workers performing state-selected direct current slice imaging experiments.[14] This has been recently used in the research group of Patwari in order to study the effect of different types of substituents on the photoreaction.[2,3] Nitrobenzene can indeed photorelease NO with both high and low translational energies, and this experimental fact is taken as proof that the photoreaction can occur according to two different mechanisms. Both the study of Lee, Ni, and co-workers and the study of Suits and co-workers proposed that the fast component is formed on the T_1 surface passing through the formation of an oxaziridine ring. Suits and co-workers also proposed that the slower NO molecules are the result of a roaming mechanism along the S_0 surface, initially leading to the nitrite isomer. The two mechanisms can be related to the intramolecular rearrangement and dissociation-recombination mechanisms originally proposed by Chapman et. al for the photorelease of NO in nitrated polycyclic aromatic hydrocarbons (see Scheme 1).[17] The recent work of Patwari based on the

Received: December 9, 2023
Revised: February 13, 2024
Accepted: February 14, 2024

Scheme 1. Photorelease Mechanism of NO According to (a) the Intramolecular Rearrangement Mechanism, (b) the Roaming Mechanism, and (c) the Dissociation-Recombination Mechanism

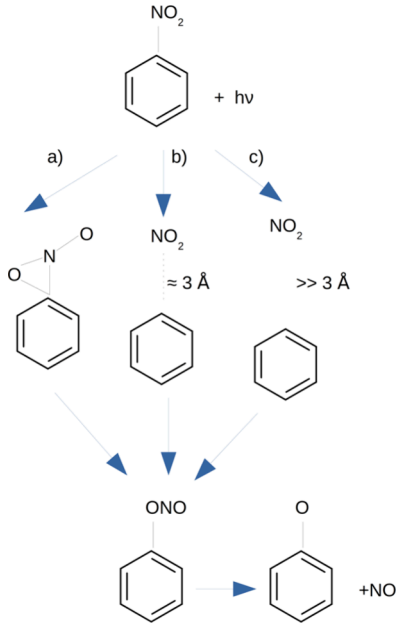

exploration of a two-dimensional model of the T_1 potential energy surface (PES) (the C−NO_2 and C−ONO bond distances) supports such a vision, concluding than the dynamics on the T_1 state acts as a doorway between the roaming and nonroaming mechanisms. Performing ab initio CASSCF and CASPT2 computations and classical CASSCF dynamics, we previously put into doubt the importance of roaming in the photorelease of NO, showing how different regions of the same T_1/S_0 seam of intersection describing an oxaziridine ring can indeed lead to NO molecules with as much as 0.7 eV difference in their corresponding translational energy.[15]

With the present contribution, we are proposing a mechanism for the photoinduced release of NO_2 on the triplet manifold and show how along such a process a possible decay to the S_0 surface can indeed result in the nitro-to-nitrite photoisomeriazion through a roaming mechanism. The work is based on ab initio CASSCF[18] and CASPT2[19] and DFT computations along with CASSCF classical dynamics simulations. Over the years, the description of the electronic structure of nitrobenzene, and of a nitroaromatics system in general, has proven to be particularly challenging.[20−25] As active space, we employed mostly the well-tested 14 electrons in 11 orbital space, although the final results were obtained including also the sigma electrons and orbitals describing the C−NO_2 bond, globally resulting in a CAS(16,13) space (see Figure S1).[22,23] All wave function computations were performed with OpenMolcas,[26,27] while DFT-B3LYP[28,29] calculations were made with Gaussian16.[30] Wave function calculations employed as the basis set the atomic natural orbital (ANO) of L-type contracted to C,N[4s,3p,1d]/H[2s1p],[31,32] while the 6-311++g(d,p) basis set was used for DFT computations.[33]

As reviewed above, NO_2 has been described as the main product of nitrobenzene photochemistry in all but one study. In a previous contribution, we suggested that such a process could be the result of the nonradiative repopulation of a hot ground state from a S_1/S_0 conical intersection. As this is characterized by a much shorter C−NO_2 bond length than the S_0 minimum (1.241 and 1.476 Å, respectively), during the evolution back to the S_0 minimum, it can carry on along the C−NO_2 stretching direction and eventually dissociate.[22] Despite the plausibility of the hypothesis, CASSCF and CASPT2 classical dynamics from the mentioned S_1/S_0 region along the S_0 surface, even if initially evolving toward structures having C−NO_2 distances as long as 1.9 Å, end up in the nitrobenzene S_0 minimum, consequently proving the tendency of the S_0 state to evolve to the nitrobenzene structure.

Since NO_2 formation will have to pass to C−NO_2 dissociation, we asked ourselves which electronic state is favored (i.e., stabilized) by such a deformation, with the logical answer being the state describing a $\sigma\sigma^*$ excitation of the C−NO_2 bond. For the moment, we will focus on the triplet states. We then computed the excited state energies of the four lowest triplet states for a series of geometries obtained by systematically elongating the C−NO_2 bond from the CASPT2 ground state minimum, where such a bond is equal to 1.47 Å, up to 2.15 Å (see Table 1, Figure S2, and Table S1). At a C−NO_2 distance of 2.0 Å, the state describing the $\sigma\sigma^*$ excitation of the C−NO_2 bond appears among the computed states at an energy of 4.65 eV with respect to the ground state in its minimum. This indicates that the $\sigma\sigma^*$ state is probably too high in energy in the ground state minimum and thermally accessible structures to be directly involved in the NO_2 photorelease experimentally detected after 280−222 nm (4.43−5.58 eV) excitation. Regarding the other triplet states, all of them get destabilized by the C−NO_2 elongation, although the $^3(n_B\pi^*)$ state (following the nomenclature of ref 22, see Figure S3 of that publication) is the one that has the smallest increase in energy (see Table 1 and Figure S2). In fact, the $^3(n_B\pi^*)$ state passes from being the T_4 at the Franck−Condon region, to be the lowest triplet state, beside the $\sigma\sigma^*$, when the C−NO_2 distance is equal to 2.15 Å. Looking at the n_B orbital (see Figures S1 and S3), we can see that it indeed partially describes a σ orbital on the C−NO_2 bond, which consequently justifies the smaller destabilization suffer by the $^3(n_B\pi^*)$ state.

Table 1. CASPT2(16,13) Energies (eV) of the Low-Lying Triplet States at the First and Last Point Computed along the C−NO_2 Scan from the Ground State Minimum Together with Their Energy Difference (ΔE, eV)[a]

	energy (eV)[a]		
State[b]	C1N7 = 1.47 Å	C1N7 = 2.15 Å	ΔE
$^3(n_A\pi^*)$	3.22	-	-
$^3(\pi_O\pi^*)$	3.45	5.70	2.25
$^3(L_a\pi\pi^*)$	3.67	5.67	2.00
$^3(n_B\pi^*)$	3.88	5.61	1.73
$^3(\sigma\sigma^*)$	-	4.07	-

[a]All energies at all geometries composing the scan are reported in Figure S2 and Table S1. All the reported values refer to the ground state energy in its minimum. [b]State nomenclature as in ref 22.

While the destabilization of some triplet states could have already been predicted from their previously published equilibrium structures,[22] no such information was available for the $^3(n_B\pi^*)$ state. We thus performed a CASSCF(14,11) optimization of this state, obtaining a minimum characterized

https://doi.org/10.1021/acs.jpclett.3c03457
J. Phys. Chem. Lett. 2024, 15, 2216−2221

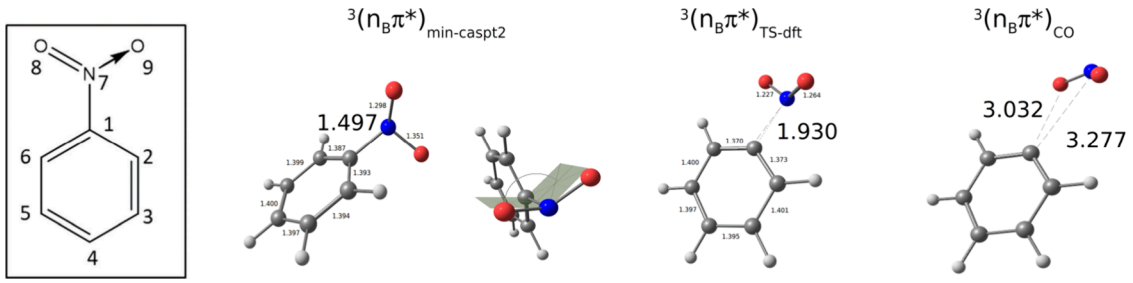

Figure 1. Key geometries of nitrobenzene. Bond lengths are reported in Å. In the inset are displayed the nitrobenzene structure and atom labeling.

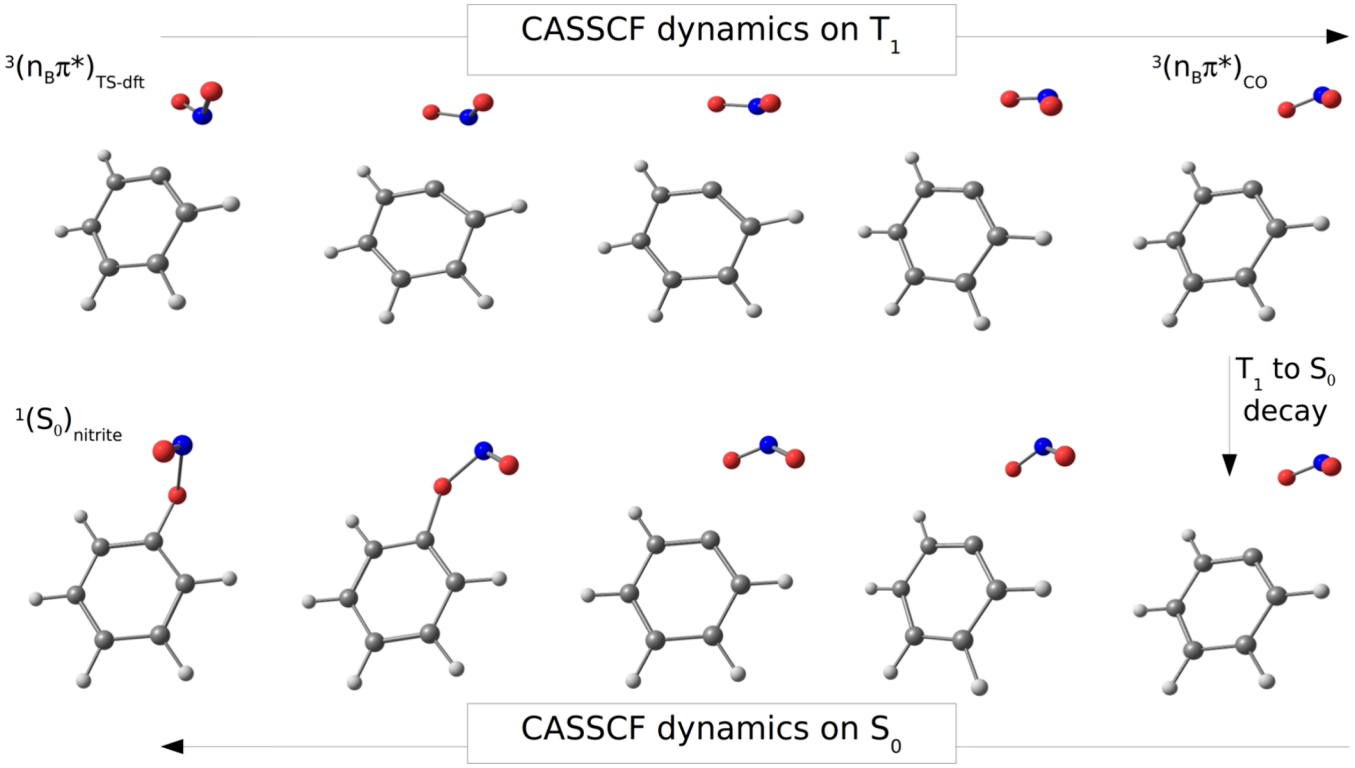

Figure 2. Geometrical evolution along the T_1 surface from the $^3(n_B\pi^*)_{TS\text{-}dft}$ to the $^3(n_B\pi^*)_{CO}$ structure, and subsequent evolution from the latter structure along the S_0 surface toward the nitrite isomer.

by a C−NO_2 distance of 1.449 Å. Since dynamic correlation has already proved to be key in the determination of reliable structural parameters for the ground state minimum of nitrobenzene, the CASSCF(14,11) $^3(n_B\pi^*)$ minimum was numerically reoptimized at the CASPT2(14,11) level. The resulting structure, hereafter $^3(n_B\pi^*)_{min\text{-}caspt2}$, is actually the first and only point obtained along a numerical CASPT2-(14,11) minimum energy path (MEP) from the CASSCF-(14,11) minimum, from which the further evolution of the $^3(n_B\pi^*)$ state we were unable to describe at the same level of theory. The $^3(n_B\pi^*)_{min\text{-}caspt2}$ structure is however characterized by a single numerical CASPT2 imaginary frequency of 47 cm^{-1} and can consequently be indeed considered as a CASPT2 minimum but constrained on the MEP hypersphere. More importantly, at the $^3(n_B\pi^*)_{min\text{-}caspt2}$ geometry, the C−NO_2 distance is equal to 1.497 Å, which is indeed the largest C−NO_2 distance of all previously characterized minima, both singlet and triplet. Additionally, the nitro group is significantly rotated with respect to the plane of the ring and describes a substantial pyramidalization (see Figure 1). Regarding its energy position, at the $^3(n_B\pi^*)_{min\text{-}caspt2}$ structure the $^3(n_B\pi^*)$ state is the T_3 state, 0.27 and 0.36 eV above the T_2 and T_1 states, respectively.

In order to further study the $^3(n_B\pi^*)$ state along the C−NO_2 stretching coordinate, we resort to using DFT calculations and ran a series of transition state (TS) optimizations on the triplet manifold starting from geometries displaying a significant elongation of the C−NO_2 bond. A B3LYP DFT transition state on the T_1 PES describing the dissociation of the NO_2 bond was obtained, hereafter $^3(n_B\pi^*)_{TS\text{-}dft}$ (see Figure 1). The only imaginary frequency characterizing this structure is equal to 463 cm^{-1} and indeed describes the NO_2 dissociation (see Figure S4). From the analysis of the corresponding DFT electron density and orbitals and performing a TDDFT computation, the T_1 state at the characterized TS geometry has indeed a marked $^3(n_B\pi^*)$ character (see Figure S5). Different attempts to obtain such TS at the CASSCF and CASPT2 level were unsuccessful.

The CASSCF and CASPT2 energies at the $^3(n_B\pi^*)_{TS\text{-}dft}$ structure were computed enlarging the active space to 16 electrons in 13 orbitals, to account for the $\sigma\sigma^*$ system of the breaking C−NO_2 bond (see Figure S1). The use of such an

https://doi.org/10.1021/acs.jpclett.3c03457
J. Phys. Chem. Lett. 2024, 15, 2216−2221

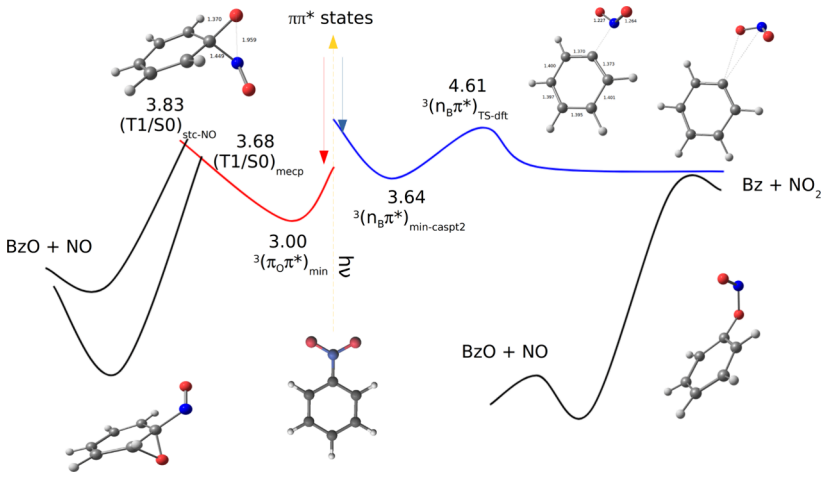

Figure 3. Schematic representation of the main photochemical routes for nitrobenzene. All the reported CASTP2(16,13) energies (eV) refer to the ground state energy at its minimum. On the right side, the here-described new paths are depicted, while on the left side the paths described in ref 15 are presented.

enlarged (16,13) active space is also supported by previous computations on the dissociation process.[22,23] At both the CASSCF(16,13) and CASPT2(16,13) level, the $^3(n_B\pi^*)$ state is the lowest triplet state at the $^3(n_B\pi^*)_{TS\text{-}dft}$ structure, while at the $^3(n_B\pi^*)_{min\text{-}caspt2}$ geometry, it is the T_3 state. Despite that, the CASPT2(16,13) energy of the $^3(n_B\pi^*)$ state is 0.27 eV lower in energy at the $^3(n_B\pi^*)_{min\text{-}caspt2}$ structure with respect to the $^3(n_B\pi^*)_{TS\text{-}dft}$ geometry, in agreement with the minimum nature of the former point. In order to better evaluate the PES separating the $^3(n_B\pi^*)_{min\text{-}caspt2}$ and $^3(n_B\pi^*)_{TS\text{-}dft}$ points, a CASPT2(16,13) LIIC calculation connecting the two structures was performed, resulting in an energy barrier for the evolution from the former to the latter of 0.97 eV (see Figure S6).

From the $^3(n_B\pi^*)_{TS\text{-}dft}$, the subsequent evolution of the $^3(n_B\pi^*)$ state was characterized by both performing CASSCF(14,11) MEP calculations and running CASSCF(14,11) dynamics (energy along the trajectory shown in Figure S7). In both cases, the system evolves toward complete NO_2 dissociation, so we can conclude that the population of the $^3(n_B\pi^*)$ state, the decay to its corresponding minimum, and the subsequent evolution to the $^3(n_B\pi^*)_{TS\text{-}dft}$ structure surmounting the upper bound energy barrier of 0.97 eV, constitutes a plausible mechanism for the photoinduced formation of NO_2 in nitrobenzene.

A frustrated NO_2 dissociation would be part of the roaming mechanism for the nitro-to-nitrite photoisomerization. We then ask ourselves if somehow along the described NO_2 photorelease process the system could instead follow a nondissociative path toward the formation of the nitrite species. Looking at the CASSCF(14,11) dynamics on the T_1 surface from the $^3(n_B\pi^*)_{TS\text{-}dft}$ structure, it is possible to observe that the dissociating NO_2 fragment rotates in such a way that the orientation of the nitro group with respect to the aromatic ring is inverted. That means that along the dissociation path the system describes a series of geometries for which the oxygen atoms are closer to the carbon atom of the aromatic ring previously attached to the nitrogen atom than the nitrogen atom itself. The phenomenon is displayed in Figure 2, together with a representative geometry, hereafter $^3(n_B\pi^*)_{CO}$, where indeed the C1O8 distance is significantly smaller than the C1N7 (3.032 and 3.277 Å, respectively, see Figure 1). These values are however large enough to describe a predissociation status, and indeed, in the $^3(n_B\pi^*)_{CO}$ structure, the T_1 and S_0 states, both describing an unpaired electron on each fragment, are very close in energy (0.27 eV). Such a situation will, in principle, allow transfer of population from T_1 to S_0, although the two display a low spin−orbit coupling of 0.75 cm^{-1} as a result of their common nature. From the latter, CASSCF(14,11) dynamics on the S_0 surface display indeed a peculiar behavior. At first, the system neither continues toward dissociation nor returns to a single bonded structure, while after around 150 fs, it abruptly decays toward nitrite formation (see Figure S8). We can then hypothesize that the key event that determines if the system will either photorelease NO_2 or photoisomerize is the passage from the T_1 to the S_0 state along the NO_2 dissociation process. It is also important to note when such a T_1 to S_0 decay takes place, since in the case where population transfer occurs at a geometry characterized by a shorter C1N7 than C1O distance, the ground state will actually return to the initial nitrobenzene structure, then globally describing a nonphotoreactive decay.

In summary, we have here characterized a possible mechanism of the photorelease of NO_2 in nitrobenzene. The process occurs on the triplet manifold, and the key protagonist is the triplet $^3(n_B\pi^*)$, which is the state among the accessible low-lying excited states that is least destabilized by the C−NO_2 stretching. From its minima, already characterized by a relatively large C−NO_2 bond length, the system can further evolve toward NO_2 dissociation, surmounting an energy barrier of at most 0.97 eV. Along the dissociation process, a combination of the reorientation undergone by the NO_2 fragment together with the approach of the complete dissociation limit where T_1 and S_0 are degenerate allows the decay from the former to the latter state, which instead of dissociating tends to react back forming either the nitrite or the nitro isomer. In the former case, the subsequent thermal release of NO will complete the roaming photorelease of NO in nitrobenzene, actually being the photoactivated and roaming part of the process the formation of the nitrite isomer.

Additionally, we attempted to evaluate whether a similar process could also occur entirely along the singlet manifold through the singlet $^1(n_B\pi^*)$ state and obtained that much

https://doi.org/10.1021/acs.jpclett.3c03457
J. Phys. Chem. Lett. 2024, 15, 2216−2221

higher energies are required and that the S_0 always tends toward a bonded structure.

At this point, it is worth putting into comparison the current results with the previous picture. Figure 3 is an attempt in this direction, showing the emerging global photochemical landscape of nitrobenzene based on current and previous outcomes (see also Figure S9 where the energies are given in kcal/mol).[15] On the right side of Figure 3, the newly described paths leading to NO_2 formation are depicted along with the related roaming mechanism, which results first in the nitrite isomer and then the release of NO. The left side of Figure 3 reports the previously characterized paths passing from the T_1/S_0 oxaziridine-like singlet triplet crossing regions and leading respectively to the direct release of NO and to the production of NO after first forming an epoxide structure. The previously characterized roaming-like path is not reported, now replaced by the new roaming mechanism described here.

Finally, it is always important to keep in mind the limitations of the proposed model. Some of the results are based on a single zero-velocity CASSCF classical dynamics simulation. Although in the present contribution we are not aiming at quantitative results, still drawing a conclusion on the basis of a single trajectory can be misleading, since it would not be able to capture possible significant dynamics effects that only an ensemble of trajectories will be able to show. We then decided to reproduce the results using a purely static approach, computing MEPs. In particular, a MEP calculation starting from the $^3(n_B\pi^*)_{TS\text{-}dft}$ geometry on the T_1 surface has been performed, which, similarly to the corresponding dynamics, evolves toward NO_2 formation, although describing a less pronounced rotation of the NO_2 fragment. At the ninth point of the MEP, hereafter $^3(n_B\pi^*)_{CO\text{-}mep}$, the C1N7 and C1O8 distances are equal to 3.018 and 3.031 Å, respectively, and the energy gap between S_0 and T_1 is equal to 0.09 eV. This energy difference will even better justify a possible T_1 to S_0 decay than the ones characterizing the $^3(n_B\pi^*)_{CO}$ geometry (0.27 eV). From this MEP point, the computation of both CASSCF(14,11) dynamics and MEP on the S_0 surfaces ended in the nitrite isomer, consequently supporting the proposed mechanism on the basis of static calculations.

■ ASSOCIATED CONTENT

Supporting Information

The Supporting Information is available free of charge at https://pubs.acs.org/doi/10.1021/acs.jpclett.3c03457.

Active space orbitals, CASPT2(16,13) energies of the lowest triplet states, description of the nature of the $^3(n_B\pi^*)$ state, imaginary frequency at the TS, CASSCF(14,11) energies of T_1 and S_0 along the performed dynamics, schematic representation of the main photochemical routes (using kcal/mol), and Cartesian coordinates of the optimized points (PDF)

Transparent Peer Review report available (PDF)

■ AUTHOR INFORMATION

Corresponding Author

Angelo Giussani − *Instituto de Ciencia Molecular, Universitat de València, ES-46071 Valencia, Spain;* orcid.org/0000-0002-9452-7641; Email: Angelo.Giussani@uv.es

Author

Graham A. Worth − *Department of Chemistry, University College London, London WC1H 0AJ, U.K.;* orcid.org/0000-0002-2044-4499

Complete contact information is available at: https://pubs.acs.org/10.1021/acs.jpclett.3c03457

Notes

The authors declare no competing financial interest.

■ ACKNOWLEDGMENTS

The financial support by EPSRC Programme Grant EP/V026690/1 is acknowledged. The financial support by the MCIN/AEI of Spain (projects PID2021-128569NB-I00 and CEX2019-000919-M, funded by MCIN/AEI/10.13039/501100011033 and by "ERDF A way of making Europe") and the Generalitat Valenciana (MFA/2022/017) is acknowledged. The MFA/2022/017 project is a part of the Advanced Materials programme supported by the MCIN with funding from the European Union NextGenerationEU (PRTR-C17.I1) and by Generalitat Valenciana.

■ REFERENCES

(1) Crane, S. W.; Garrow, M.; Lane, P. D.; Robertson, K.; Waugh, A.; Woolley, J. M.; Stavros, V. G.; Paterson, M. J.; Greaves, S. J.; Townsend, D. The Value of Different Experimental Observables: A Transient Absorption Study of the Ultraviolet Excitation Dynamics Operating in Nitrobenzene. *J. Phys. Chem. A* **2023**, *127* (31), 6425−6436.

(2) Bejoy, N. B.; Roy Chowdhury, P.; Patwari, G. N. Modulating the Roaming Dynamics for the NO Release in Ortho-Nitrobenzenes. *J. Phys. Chem. Lett.* **2023**, *14* (11), 2816−2822.

(3) Bejoy, N. B.; Patwari, G. N. Photodegradation of Flutamide and Halogen Derivatives of Nitrobenzotrifluoride: The NO Release Channel. *J. Phys. Chem. A* **2023**, *127* (34), 7168−7174.

(4) Hegazy, K.; Cryan, J.; Li, R.; Lin, M.-F.; Moore, B.; Nunes, P.; Shen, X.; Weathersby, S.; Yang, J.; Wang, X.; Wolf, T.. Investigating Dissociation Pathways of Nitrobenzene via Mega-Electron-Volt Ultrafast Electron Diffraction. *arXiv:2308.03996*, 2023.

(5) Liu, R.; Zhang, Z.; Yan, L.; Yang, X.; Zhu, Y.; Su, P.; Song, H.; Wang, Z. The Influence of Hydrogen Bonds on the Roaming Reaction. *J. Phys. Chem. Lett.* **2023**, *14* (41), 9351−9356.

(6) Thurston, R.; Brister, M. M.; Tan, L. Z.; Champenois, E. G.; Bakhti, S.; Muddukrishna, P.; Weber, T.; Belkacem, A.; Slaughter, D. S.; Shivaram, N. Ultrafast Dynamics of Excited Electronic States in Nitrobenzene Measured by Ultrafast Transient Polarization Spectroscopy. *J. Phys. Chem. A* **2020**, *124* (13), 2573−2579.

(7) Rodríguez-Córdoba, W.; Gutiérrez-Arzaluz, L.; Cortés-Guzmán, F.; Peon, J. Excited State Dynamics and Photochemistry of Nitroaromatic Compounds. *Chem. Commun.* **2021**, *57* (92), 12218−12235.

(8) Brill, T. B.; James, K. J. Kinetics and Mechanisms of Thermal Decomposition of Nitroaromatic Explosives. *Chem. Rev.* **1993**, *93* (8), 2667−2692.

(9) Nakagawa, H.; Hishikawa, K.; Eto, K.; Ieda, N.; Namikawa, T.; Kamada, K.; Suzuki, T.; Miyata, N.; Nabekura, J. I. Fine Spatiotemporal Control of Nitric Oxide Release by Infrared Pulse-Laser Irradiation of a Photolabile Donor. *ACS Chem. Biol.* **2013**, *8* (11), 2493−2500.

(10) Nelson, P. O.; Thayumanavan, P.; Azizian, M. F.; Williamson, K. J. Evaluation Methodology for Environmental Impact Assessment of Industrial Wastes Used as Highway Materials: An Overview with Respect to U.S. EPA's Environmental Risk Assessment Framework. *Water Pollut.* **2005**, *1*, 271−291.

(11) Galloway, D. B.; Bartz, J. A.; Huey, L. G.; Crim, F. F. Pathways and Kinetic Energy Disposal in the Photodissociation of Nitrobenzene. *J. Chem. Phys.* **1993**, *98* (3), 2107−2114.
(12) Lin, M. F.; Lee, Y. T.; Ni, C. K.; Xu, S.; Lin, M. C. Photodissociation Dynamics of Nitrobenzene and O-Nitrotoluene. *J. Chem. Phys.* **2007**, *126* (6), 064310.
(13) He, Y.; Gahlmann, A.; Feenstra, J. S.; Park, S. T.; Zewail, A. H. Ultrafast Electron Diffraction: Structural Dynamics of Molecular Rearrangement in the NO Release from Nitrobenzene. *Chem. - An Asian J.* **2006**, *1* (1−2), 56−63.
(14) Hause, M. L.; Herath, N.; Zhu, R.; Lin, M. C.; Suits, A. G. Roaming-Mediated Isomerization in the Photodissociation of Nitrobenzene. *Nat. Chem.* **2011**, *3* (12), 932−937.
(15) Giussani, A.; Worth, G. A. How Important Is Roaming in the Photodegradation of Nitrobenzene? *Phys. Chem. Chem. Phys.* **2020**, *22* (28), 15945−15952.
(16) Giussani, A.; Worth, G. A. On the Photorelease of Nitric Oxide by Nitrobenzene Derivatives: A CASPT2//CASSCF Model. *J. Chem. Phys.* **2022**, *157* (20), 204301.
(17) Chapman, O. L.; Heckert, D. C.; Reasoner, J. W.; Thackaberry, S. P. Photochemical Studies on 9-Nitroanthracene1. *J. Am. Chem. Soc.* **1966**, *88* (23), 5550−5554.
(18) Roos, B. O. The Complete Active Space SCF Method in a Fock-matrix-based Super-CI Formulation. *Int. J. Quantum Chem.* **1980**, *18* (S14), 175−189.
(19) Andersson, K.; Malmqvist, P. Å.; Roos, B. O. Second-Order Perturbation Theory with a Complete Active Space Self-Consistent Field Reference Function. *J. Chem. Phys.* **1992**, *96* (2), 1218−1226.
(20) Quenneville, J.; Greenfield, M.; Moore, D. S.; McGrane, S. D.; Scharff, R. J. Quantum Chemistry Studies of Electronically Excited Nitrobenzene, TNA, and TNT. *J. Phys. Chem. A* **2011**, *115* (44), 12286−12297.
(21) Mewes, J. M.; Jovanović, V.; Marian, C. M.; Dreuw, A. On the Molecular Mechanism of Non-Radiative Decay of Nitrobenzene and the Unforeseen Challenges This Simple Molecule Holds for Electronic Structure Theory. *Phys. Chem. Chem. Phys.* **2014**, *16* (24), 12393−12406.
(22) Giussani, A.; Worth, G. A. Insights into the Complex Photophysics and Photochemistry of the Simplest Nitroaromatic Compound: A CASPT2//CASSCF Study on Nitrobenzene. *J. Chem. Theory Comput.* **2017**, *13* (6), 2777−2788.
(23) Soto, J.; Algarra, M. Electronic Structure of Nitrobenzene: A Benchmark Example of the Accuracy of the Multi-State CASPT2 Theory. *J. Phys. Chem. A* **2021**, *125* (43), 9431−9437.
(24) Giussani, A. Toward the Understanding of the Photophysics and Photochemistry of 1-Nitronaphthalene under Solar Radiation: The First Theoretical Evidence of a Photodegradation Intramolecular Rearrangement Mechanism Involving the Triplet States. *J. Chem. Theory Comput.* **2014**, *10* (9), 3987−3995.
(25) Giussani, A.; Worth, G. A. Similar Chemical Structures, Dissimilar Triplet Quantum Yields: A CASPT2Model Rationalizing the Trend of Triplet Quantum Yields in Nitroaromatic Systems. *Phys. Chem. Chem. Phys.* **2019**, *21* (20), 10514−10522.
(26) Fdez. Galván, I.; Vacher, M.; Alavi, A.; Angeli, C.; Aquilante, F.; Autschbach, J.; Bao, J. J.; Bokarev, S. I.; Bogdanov, N. A.; Carlson, R. K.; Chibotaru, L. F.; Creutzberg, J.; Dattani, N.; Delcey, M. G.; Dong, S. S.; Dreuw, A.; Freitag, L.; Frutos, L. M.; Gagliardi, L.; Gendron, F.; Giussani, A.; González, L.; Grell, G.; Guo, M.; Hoyer, C. E.; Johansson, M.; Keller, S.; Knecht, S.; Kovačević, G.; Källman, E.; Li Manni, G.; Lundberg, M.; Ma, Y.; Mai, S.; Malhado, J. P.; Malmqvist, P. Å.; Marquetand, P.; Mewes, S. A.; Norell, J.; Olivucci, M.; Oppel, M.; Phung, Q. M.; Pierloot, K.; Plasser, F.; Reiher, M.; Sand, A. M.; Schapiro, I.; Sharma, P.; Stein, C. J.; Sørensen, L. K.; Truhlar, D. G.; Ugandi, M.; Ungur, L.; Valentini, A.; Vancoillie, S.; Veryazov, V.; Weser, O.; Wesołowski, T. A.; Widmark, P. O.; Wouters, S.; Zech, A.; Zobel, J. P.; Lindh, R. OpenMolcas: From Source Code to Insight. *J. Chem. Theory Comput.* **2019**, *15* (11), 5925−5964.
(27) Li Manni, G.; Fdez. Galván, I.; Alavi, A.; Aleotti, F.; Aquilante, F.; Autschbach, J.; Avagliano, D.; Baiardi, A.; Bao, J. J.; Battaglia, S.; Birnoschi, L.; Blanco-González, A.; Bokarev, S. I.; Broer, R.; Cacciari, R.; Calio, P. B.; Carlson, R. K.; Carvalho Couto, R.; Cerdán, L.; Chibotaru, L. F.; Chilton, N. F.; Church, J. R.; Conti, I.; Coriani, S.; Cuéllar-Zuquin, J.; Daoud, R. E.; Dattani, N.; Decleva, P.; de Graaf, C.; Delcey, M. G.; De Vico, L.; Dobrautz, W.; Dong, S. S.; Feng, R.; Ferré, N.; Filatov, M.; Gagliardi, L.; Garavelli, M.; González, L.; Guan, Y.; Guo, M.; Hennefarth, M. R.; Hermes, M. R.; Hoyer, C. E.; Huix-Rotllant, M.; Jaiswal, V. K.; Kaiser, A.; Kaliakin, D. S.; Khamesian, M.; King, D. S.; Kochetov, V.; Krośnicki, M.; Kumaar, A. A.; Larsson, E. D.; Lehtola, S.; Lepetit, M. B.; Lischka, H.; López Ríos, P.; Lundberg, M.; Ma, D.; Mai, S.; Marquetand, P.; Merritt, I. C. D.; Montorsi, F.; Mörchen, M.; Nenov, A.; Nguyen, V. H. A.; Nishimoto, Y.; Oakley, M. S.; Olivucci, M.; Oppel, M.; Padula, D.; Pandharkar, R.; Phung, Q. M.; Plasser, F.; Raggi, G.; Rebolini, E.; Reiher, M.; Rivalta, I.; Roca-Sanjuán, D.; Romig, T.; Safari, A. A.; Sánchez-Mansilla, A.; Sand, A. M.; Schapiro, I.; Scott, T. R.; Segarra-Martí, J.; Segatta, F.; Sergentu, D. C.; Sharma, P.; Shepard, R.; Shu, Y.; Staab, J. K.; Straatsma, T. P.; Sørensen, L. K.; Tenorio, B. N. C.; Truhlar, D. G.; Ungur, L.; Vacher, M.; Veryazov, V.; Voß, T. A.; Weser, O.; Wu, D.; Yang, X.; Yarkony, D.; Zhou, C.; Zobel, J. P.; Lindh, R. The OpenMolcas Web: A Community-Driven Approach to Advancing Computational Chemistry. *J. Chem. Theory Comput.* **2023**, *19*, 6933−6991.
(28) Becke, A. D. Density-Functional Thermochemistry. III. The Role of Exact Exchange. *J. Chem. Phys.* **1993**, *98*, 5648−5652.
(29) Lee, C.; Yang, W.; Parr, R. G. Development of the Colle-Salvetti Correlation-Energy Formula into a Functional of the Electron Density. *Phys. Rev. B* **1988**, *37*, 785.
(30) Frisch, M. J.; Trucks, G. W.; Schlegel, H. B.; Scuseria, G. E.; Robb, M. A.; Cheeseman, J. R.; Scalmani, G.; Barone, V.; Petersson, G. A.; Nakatsuji, H.; Li, X.; Caricato, M.; Marenich, A. V.; Blolino, J.; Janesko, B. G.; Gomperts, R.; Mennucci, B.; Hratchian, H. P.; Ortiz, J. V.; Izmaylov, A. F.; Sonnenberg, J. L.; Williams-Young, D.; Ding, F.; Lipparini, F.; Egidi, F.; Goings, J.; Peng, B.; Petrone, A.; Henderson, T.; Ranasinghe, D.; Zakrzewski, V. G.; Gao, J.; Rega, N.; Zheng, G.; Liang, W.; Hada, M.; Ehara, M.; Toyota, K.; Fukuda, R.; Hasegawa, J.; Ishida, M.; Nakajima, T.; Honda, Y.; Kitao, O.; Nakai, H.; Vreven, T.; Throssell, K.; Montgomery, J. A., Jr.; Peralta, J. E.; Oligaro, F.; Bearpark, M. J.; Heyd, J. J; Brothers, E. N.; Kudin, K. N.; Staroverov, V. N.; Keith, T. A.; Kobayashi, R.; Normand, J.; Ragavachari, K.; Rendell, A. P.; Burant, J. C.; Iyengar, S. S.; Tomasi, J.; Cossi, M.; Millam, J. M.; Klene, M.; Adamo, C.; Cammi, R.; Ochterski, J. W.; Martin, R. L.; Morokuma, K.; Farkas, O.; Foresman, J. B.; Fox, D. J. *Gaussian 16*, revision C.01; Gaussian, Inc.: Wallingford, CT, 2016.
(31) Widmark, P. O.; Malmqvist, P. Å.; Roos, B. O. Density Matrix Averaged Atomic Natural Orbital (ANO) Basis Sets for Correlated Molecular Wave Functions - I. First Row Atoms. *Theor. Chim. Acta* **1990**, *77*, 291−306.
(32) Pierloot, K.; Dumez, B.; Widmark, P.-O.; Roos, B. O. Density Matrix Averaged Atomic Natural Orbital (ANO) Basis Sets for Correlated Molecular Wave Functions. *Theor. Chim. Acta* **1995**, *90*, 87−114.
(33) Francl, M. M.; Pietro, W. J.; Hehre, W. J.; Binkley, J. S.; Gordon, M. S.; DeFrees, D. J.; Pople, J. A. Self-Consistent Molecular Orbital Methods. XXIII. A Polarization-Type Basis Set for Second-Row Elements. *J. Chem. Phys.* **1982**, *77*, 3654−3665.

https://doi.org/10.1021/acs.jpclett.3c03457
J. Phys. Chem. Lett. 2024, 15, 2216−2221